# Formation of Hierarchical Nanoparticle Pattern Arrays Using Colloidal Lithography and Two-Step Self-Assembly: Microspheres atop Nanospheres

Deying Xia,* Zahyun Ku, Dong Li, and S. R. J. Brueck*

*Center for High Technology Materials, University of New Mexico, 1313 Goddard, SE, Albuquerque, New Mexico 87106*

*Received September 16, 2007. Revised Manuscript Received November 3, 2007*

We report a simple approach to the fabrication of hierarchical nanoparticle arrays and film patterns using a novel combination of colloidal lithography (CL), two-step self-assembly, and reactive-ion etching (RIE). In this approach, a uniform nanoparticle film (∼15−50 nm particle diameter) is first deposited on a substrate. Then, larger (several hundred to thousands of nanometers diameter) microparticles with a different composition are self-assembled into well-ordered patterns atop the nanoparticle film. Next, reactive-ion etching is used to remove parts of the initial nanoparticle film using the upper layer of large particles as a mask. After selective removal of the remaining upper layer of large particles, hierarchical nanoparticle patterns are obtained on flat surfaces. Hexagonal patterns of small nanoparticle film arrays were easily fabricated with a monolayer of large spheres using this approach. Moreover, the shape and diameter of nanoparticle film disks depend on the etching duration while the periodicity of the self-assembled upper layer is preserved during the etching process. The profiles of the nanoparticle film patterns (pitch, thickness of film, etc.) are adjustable with the size of the large particles, thickness of nanoparticle film, and nanoparticle size. Furthermore, additional nanoparticle film patterns are possible with the use of additional layers of large particles. We have demonstrated the feasibility of this approach with both polystyrene (PS) spheres on silica nanoparticles and silica spheres on PS nanoparticles. This bottom-up approach offers a novel lithography-free method for the fabrication of patterned nanoparticle films that will be useful for material growth, biosensing, and catalysis as well as serving as a unit operation for further fabrication.

## Introduction

The fabrication of periodic nanoparticle array films is of great interest due to their size-dependent properties leading to a wide range of potential applications in biosensors[1,2] and chemical sensors,[3] optical and electronic devices,[4,5] and as templates for the growth of other nanomaterials.[6,7] A variety of techniques have been developed for the fabrication of patterned nanoparticle arrays. Among these techniques, directed self-assembly of nanoparticles onto templated substrates has been well studied, as reviewed recently.[8,9] Typically, the templates are generated with lithographic techniques such as colloidal lithography (CL), e-beam lithography, and interferometric lithography (IL), and then the nanoparticles are selectively deposited into grooves or holes via suitable deposition methods such as dip- or spin-coating.[10–13] Much of this directed self-assembly research has focused on a "bottom-up" oriented fabrication in which the particles are added to existing templates. Although this research has demonstrated flexible, well-defined patterns, there are difficulties with uniformly depositing particles into small isolated areas and with practical issues such as uniformity over large areas. Therefore, it is highly desirable to develop additional techniques that enable fabrication of large area patterns of nanoparticle films on flat surfaces with high yield, controllable thickness, and high uniformity over large areas.

Recently, we developed a "top-down" approach for the fabrication of high-quality nanoparticle patterns on flat surfaces over large areas[14,15] in which uniform nanoparticle films were deposited using spin-coating, and IL was then used to define photoresist (PR) patterns that were transferred

* Corresponding authors. E-mail: dyxia@chtm.unm.edu, brueck@chtm.unm.edu.

(1) Music, R. C.; Storhoff, J. J.; Letsinger, R. L.; Mirkin, C. A. *Nature (London)* **1996**, *382*, 607.
(2) Haes, A. J.; Chang, L.; Klein, W. L.; Van Duyne, R. P. *J. Am. Chem. Soc.* **2005**, *127*, 2264.
(3) Scott, R.; Yang, S. M.; Coombs, N.; Ozin, G. A.; Williams, D. E. *Adv. Funct. Mater.* **2003**, *13*, 225.
(4) Weissan, J. M.; Sunkara, H. B.; Tse, A. S.; Asher, S. A. *Science* **1996**, *274*, 959.
(5) Veinot, J. G. C.; Yan, H.; Smith, S. M.; Cui, J.; Huang, Q.; Marks, T. J. *Nano Lett.* **2002**, *2*, 333.
(6) Velev, O. D.; Tessier, P. M.; Lenhoff, A. M.; Kaler, E. W. *Nature (London)* **1999**, *401*, 548.
(7) Jiang, P.; Bertone, J. F.; Colvin, V. L. *Science.* **2001**, *291*, 453.
(8) Wang, D.; Mohwald, H. *J. Mater. Chem.* **2004**, *14*, 459.
(9) Gates, B.; Xu, Q.; Stewart, M.; Ryan, D.; Willson, C. G.; Whitesides, G. M. *Chem. Rev.* **2005**, *105*, 1171.
(10) Wang, D.; Mohwald, H. *Adv. Mater.* **2004**, *16*, 244.
(11) Xia, D.; Biswas, A.; Li, D.; Brueck, S. R. J. *Adv. Mater.* **2004**, *16*, 1427.
(12) Xia, D.; Brueck, S. R. J. *Nano Lett.* **2004**, *4*, 1295.
(13) Juillerat, F.; Solak, H. H.; Bowen, P.; Hofmann, H. *Nanotechnology* **2005**, *16*, 1311.
(14) Xia, D.; Li, D.; Luo, Y.; Brueck, S. R. J. *Adv. Mater.* **2006**, *18*, 930.
(15) Xia, D.; Li, D.; Zu, K.; Luo, Y.; Brueck, S. R. J. *Langmuir* **2007**, *23*, 5377.

10.1021/cm702644c CCC: $40.75 
Published on Web 01/31/2008

to the nanoparticle film layer to via etching. In this contribution, we extend this concept to a colloidal lithography approach using a two-layer deposition scheme in which small particles are deposited in a bottom layer followed by larger particles that form an etch mask for patterning the underlying layer. The large particles are then removed, leaving a 2D patterned nanoparticle array. This completely bottom-up fabrication sequence is demonstrated to produce high-quality, large-area arrays without requiring an expensive top-down lithographic apparatus.

The spin-coating driven assembly of colloidal particles is fast and inexpensive, consumes only a small volume of suspension, and is suitable for the wafer-scale batch microfabrication.[12,16,17] The spin-coating process is a simple technique than has been demonstrated to fabricate nanoparticle films with high uniformity and controllable thickness over large areas.[18,19]

CL is a powerful alternative approach to the conventional optical lithography used in the semiconductor industry. CL is a versatile, low-cost, high-throughput, parallel nanofabrication technique.[20] Single or double layers of colloidal particles have been used as masks or templates for patterned metals or polymers. The interstices among particles have been used as a space for the infiltration of new materials. After the removal of colloidal particles, an array of new materials in patterns such as triangular nanodisks is left on a substrate. For example, gold nanoparticles with tunable sizes have been fabricated with a combination of CL, reactive-ion etching (RIE), and thermal annealing.[21] With CL, nanoscale depressions with rounded bottoms (nanobowls) of new materials have been fabricated from monolayer colloidal particles with plasma etching[22] or ion-beam milling.[23] Another important application of CL is for nanopatterned material growth. In this approach, a monolayer of colloidal particles is first deposited, and then a catalyst layer is deposited with the colloidal particle film as a negative template. After removal of the particles, the desired materials such as $TiO_2$[24] and $SiO_2$[25] were grown in patterned arrays for applications in optoelectronics and biosensors.

In addition, one can exploit the properties of colloidal spheres that naturally pack into ordered arrangements and subsequently transform the colloidal spheres into nonspherical particles while maintaining the ordered arrangements of the particles. Fujimura et al.[26] and Tan et al.[27] made use of RIE to modify self-assembled 2D arrays of polystyrene microspheres into periodic nanoscale-rugged structures or a periodic non-close-packed array of nonspherical particles. Choi et al. also employed RIE to create various and complex nonspherical particles through multilayered spherical colloidal particles and orientation with CL.[28]

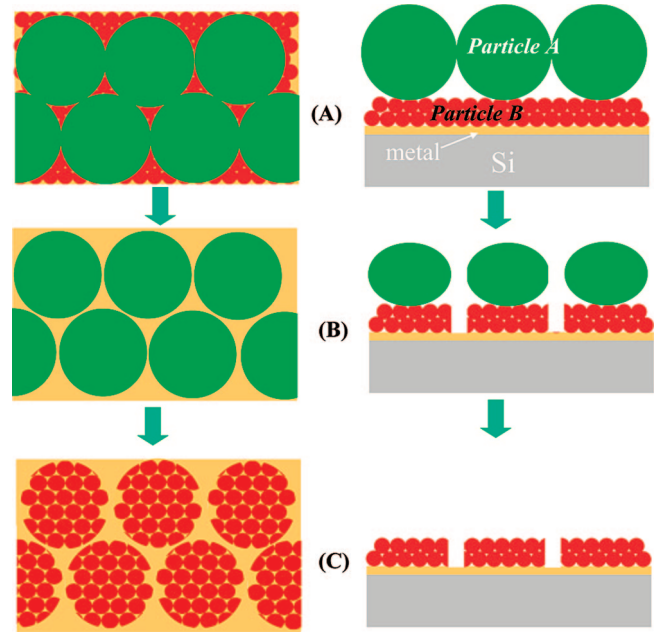


**Figure 1.** Schematic illustration of the fabrication of nanoparticle film patterns using colloidal lithography. Left column: top view; right column: side view. (A) A monolayer of self-assembled PS spheres atop a silica nanoparticle film and a thin metal film on a Si substrate. (B) After reactive ion etching of silica nanoparticle films with PS sphere mask. (C) After removal of etched PS spheres.

Here, we report a simple, inexpensive approach to combining spin-coating driven self-assembly and CL and RIE to fabricate nanoparticle film patterns with sub-micrometer periodicity. In this work, we make use of two-step self-assembly for deposition of nanoparticle films and of large colloidal particle monolayers, colloidal lithography, and RIE to define mesoscopic patterns of nanoparticles on a flat surface.

## Experimental Section

A schematic of our nanoparticle pattern fabrication process is shown in Figure 1. First, a thin metal layer was deposited on a Si substrate, and a film of small nanoparticles (particle A) was deposited by spin-coating with an aqueous colloidal suspension. The metal layer, usually ~30−50 nm thick Cr, will serve as the etch-stop layer for a subsequent reactive-ion etch (RIE) process. Both 50 and 15 nm diameter silica nanoparticles (Nissan Chemical America Corp.) were used. Typically, a ~5 wt % 50 nm silica suspension was spun at 4000 rpm for 30 s, and a ~5 wt % 15 nm silica suspension was spun at 5000 rpm for 30 s. After spin-coating, the sample was baked for 5 min at 95 °C to drive off any adsorbed water. For polystyrene (PS) nanoparticles, 100 nm diameter PS particles (Bangs Laboratories, Inc.), a ~5 wt % suspension was spin-deposited at 4000 rpm for 30 s.

Next, large PS or silica spheres (particle B) were spun on top of the film of small nanoparticles using a suitable diluted suspension to form a monolayer of large particles. The spin-coating program was typically spin-coating at 800 rpm for 10 s and 4000 rpm for

(16) Ozin, G. A.; Yang, S. M. *Adv. Funct. Mater.* **2001**, *11*, 95.
(17) Wang, D.; Mohwald, H. *Adv. Mater.* **2004**, *16*, 244.
(18) Jiang, P.; McFarland, M. F. *J. Am. Chem. Soc.* **2004**, *126*, 13778.
(19) Jiang, P.; McFarland, M. F. *J. Am. Chem. Soc.* **2005**, *127*, 3710.
(20) Haynes, C. L.; Van Duyne, R. P. *J. Phy. Chem. B* **2001**, *105*, 5599.
(21) Tan, B. J. Y.; Sow, C. H.; Koh, T. S.; Chin, K. C.; Wee, A. T. S.; Ong, C. K *J. Phys. Chem. B* **2005**, *109*, 11100.
(22) Jiang, P. *Chem. Commun.* **2005**, 1699.
(23) Wang, X. D.; Graugnard, E.; King, J. S.; Wang, Z. L.; Summers, C. J. *Nano Lett.* **2004**, *4*, 2223.
(24) Wang, X. D.; Summers, C. J.; Wang, Z. L. *Nano Lett.* **2004**, *4*, 423.
(25) An, X.; Meng, G.; Wei, Q.; Kong, M.; Zhang, L. *J. Phys. Chem. B* **2006**, *110*, 222.
(26) Fujimura, T.; Tamura, T.; Itoh, T.; Haginaya, C.; Komori, Y.; Koda, T. *Appl. Phy. Lett.* **2001**, *78*, 1478.
(27) Tan, B. J.-Y.; Sow, C.-H.; Lim, K.-Y.; Cheong, F.-C.; Chong, G.-L.; Wee, A. T.-S.; Ong, C.-K *J. Phys. Chem. B* **2004**, *108*, 18575.
(28) Choi, D. G.; Yu, H. K.; Jang, S. G.; Yang, S. M. *J. Am. Chem. Soc.* **2004**, *126*, 7019.

30 s. The large spheres serve as a soft (erodible) mask in the RIE step. After the second spin coating, a self-ordered film of large spheres (particle B), in most cases in a somewhat defected hexagonal close-packed array, is arranged atop a self-ordered film of small spheres (particle A), as shown in Figure 1A. Because of the large disparity in particle sizes, there is no correlation between the positions of the particles in the two films.

Anisotropic RIE was used to etch away the nanoparticle film through the voids between the large spheres; i.e., the top film provided a mask for the etching of the bottom film. The RIE conditions were sufficiently gentle that the ordered structure of the top (mask) film was undisturbed during the etching.[28] The reactive plasma easily diffused through the interstices between the larger particles and etched the exposed nanoparticle film regions while the nanoparticle film regions underneath the large spheres were protected from etching. A mixture of $O_2$ and $CHF_3$ (50:130) was used to etch the silica nanoparticles at a power of 100 W while $O_2$ was used to etch the PS nanoparticles at a power of 25 W. The duration of RIE was varied from 1.5 to 10 min. Because of the inclusion of $O_2$ in the RIE gas mixture, the PS spheres were partially etched as well, as shown in Figure 1B. After the RIE step, a piranha solution or a high-temperature calcination (400 °C, 2 h) were used to remove the partially etched PS particles of the top layer to form nanoparticle patterns on flat surfaces. For the silica on PS case, dilute HF (~1%) solution was applied to remove the silica spheres, as shown in Figure 1C. The samples were studied using scanning electron microscopy (SEM, JEOL 6400F).

## Results and Discussion

First we discuss the case of large PS spheres atop a silica nanoparticle film. Spin-coating was used to deposit the silica nanoparticle film on a Si substrate with a thin metal layer. The spin-coating-driven self-assembly of silica nanoparticle films was easy, fast, and controllable for film thickness and uniformity over a large area even though it was relatively difficult to form a single monolayer thick nanoparticle film, partially due to the large size distribution of the commercially available silica nanoparticles.[14] The thickness of the silica nanoparticle film was controlled by experimental parameters such as spin speed, suspension concentration, cycles of spin-coating, etc. In a typical case, a roughly 100 nm thick silica nanoparticle film was achieved at 4000 rpm for 30 s for a ~5 wt % 50 nm silica suspension (two to three particles thick).

After deposition of the nanoparticle film, larger colloidal spheres were deposited on top of the film with an appropriate deposition approach. There are two basic requirements to obtain the desired nanoparticle patterns using this approach: (1) compositions of the large micro- or nanoparticles and the small nanoparticles should be different enough that the large particles can serve as a mask layer during the etching of the bottom layer and can be selectively removed after the etching step; (2) the diameter of large particles should be at least 5 times larger than that of the small particles to produce obvious patterns in nanoparticle layer and to avoid correlation between the particle positions in the two layers.

Spin-coating is a rapid, facile technique to form 2D PS arrays. Dip-coating is another choice for deposition of a 2D PS array; however, it takes long time and is difficult to find the appropriate conditions.[29] Many approaches for the deposition of 2D colloidal spheres on flat surface have been developed; for example, convective assembly (also defined as a vertical deposition method)[30] and modified connective assembly with confinement between two substrates[31,32] are additional techniques.

In our experiment, we employed spin-coating to deposit monolayer and double-layer PS spheres atop silica nanoparticle films. The spin-coating program is critical in forming films with good uniformity over a large area.[16] We optimized the experimental conditions for a PS monolayer film over a large area by adjusting the spin-coating program. The best result was obtained with spin-coating at 800 rpm for 10 s and 4000 rpm for 30 s. Defect-free domains were in the range of several to a few hundred square micrometers ($\mu m^2$). A hexagonal close-packed 1000 nm particle diameter PS monolayer was obtained as seen in Figure 2A. These monolayer PS spheres are well-ordered (see Supporting Information Figure S1A). The underlying nanoparticle film is evident in the region of a point defect in the masking film (Figure 2B). From the side view, Figure 2C, it is clear that the monolayer of PS spheres touch the ~2 nanoparticle deep, 50 nm diameter silica nanoparticle film (red arrow). The 50 nm thick metal layer is indicated by the green arrow.

The deposition morphologies of both the nanoparticle underlayer and the microparticle overlayer are affected by many experimental parameters such as the pH and ionic strength of the colloidal suspensions.[11,33] Our experiments used commercial, as-received particle suspensions diluted with deionized water so that the nanoparticle suspension had a low ionic strength and a moderate pH. We will investigate the effect of pH and ion strength on pattern formation in future work.

Next, RIE was used to etch the nanoparticle film with the PS spheres as a "mask". A gas mixture of $CHF_3$ and $O_2$ is effective for etching the silica layer and the silicon substrate. Without the metal etch-stop layer, the etching continues into the substrate, resulting in "micro/nanoplatforms". This gas mixture also results in oxyfluoride ions, which are a highly reactive etching agent for the PS.[27] In our experiment, we found that the reactive species directed normally onto the sample surface played a dominant role in the etching process. As a result, the PS spheres and silica nanoparticles are preferentially etched perpendicular to the substrate. During the etching, the symmetric PS spheres were transformed into smaller anisotropic particles. SEM images in Figure 2D,F show the etched profiles after 6 min RIE duration. Under these conditions, the PS particles are still at their original hexagonal close-packed positions, but the film is no longer close-packed as a result of the partial etching of the PS. The silica nanoparticle film is completly etched away in the original interstices and point defect regions, as shown in

(29) Nam, H. J.; Jung, D.-Y.; Yi, G.-R.; Choi, H. *Langmuir* **2006**, *22*, 7358.
(30) Jiang, P.; Bertone, F.; Hwang, K. S.; Colvin, V. L. *Chem. Mater.* **1999**, *11*, 2132.
(31) Kim, M. H.; Im, S. H.; Park, O. O. *Adv. Funct. Mater.* **2005**, *15*, 1329.
(32) Kim, M. H.; Choi, H. K.; Park, O. O.; Im, S. H. *Appl. Phy. Lett.* **2006**, *88*, 143127.
(33) Yake, A. M.; Snyder, C. E.; Velegol, D. *Langmuir* **2007**, *23*, 9069.

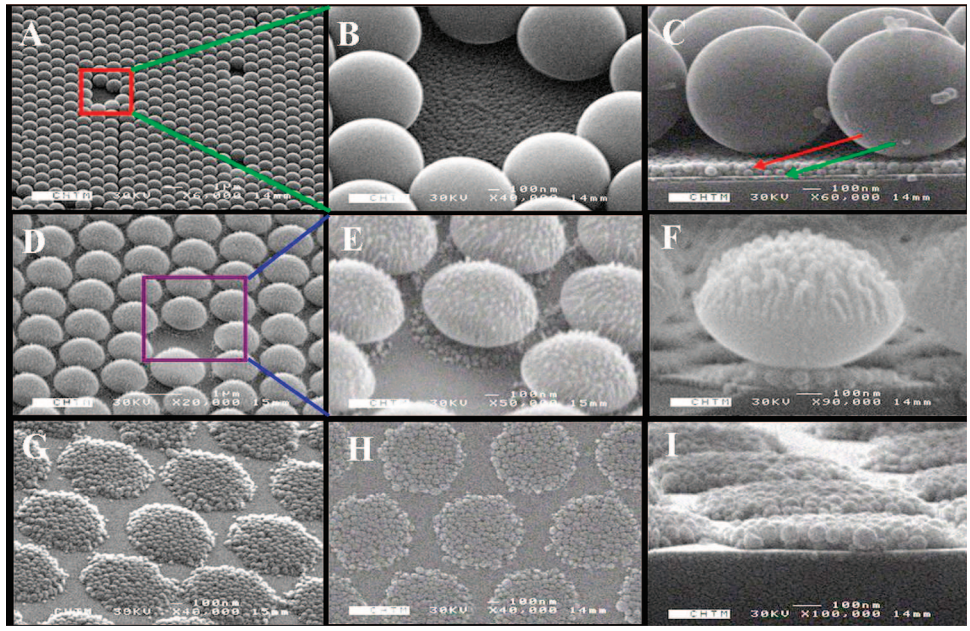


**Figure 2.** SEM images of a monolayer of 1000 nm PS spheres atop a 50 nm silica nanoparticle film: (A−C) self-assembled PS on silica nanoparticle film, (D−F) after 6 min RIE, (G−I) after removal of PS spheres. Tilted view (45°): (A), (B), (D), (E), (G); top view: (H); side view: (C), (F), (I).

Figure 2E. From a magnified side view (Figure 2F), we can conclude that the nanoparticle film under the shadow of the etched PS particles is not removed. The upper surface of etched PS particle is erose while the bottom surface retains its original smoothness. Tan et al. investigated the profile evolution of PS particles during RIE.[27] With 6 min RIE duration, PS particle size became much smaller than original PS size and the underlying silica nanoparticle patterns are well separated. Hierarchical and heterogeneous multicomponent isolated particle arrays are formed in this step.

Both wet (immersion in piranha solution) and dry (high-temperature calcination) were used for removing the top PS particle layer. Even with the harsh piranha treatment, the fabricated nanoparticle patterned films were preserved. A gentler wet method such as immersion in $CH_2Cl_2$ or toluene[24,25] is also applicable for removing the PS particles. The high-temperature calcination (400 °C, 2 h) enhances the stability of resultant patterned nanoparticle films by inducing partial necking where the silica particles touch. After removal of etched PS particles, well-separated silica nanoparticle film islands are obtained as shown in Figure 2G−I. The nanoparticle islands are circular and well-separated. The overall pattern is hexagonal with the same period as the original PS spheres. Furthermore, the thickness and packing of silica nanoparticle in patterned regions were maintained as shown in Figure 2I. PS particle patterns are successively transferred into underlying nanoparticle film layer over a large area (see Supporting Information Figure S1C,D). Other deposition techniques for the PS mask film, such as confined convective assembly,[32] have been demonstrated over large areas with an improved uniformity and a lower density of defects than obtained with spin-coating. These characteristics would be transferred to the final nanoparticle films patterns.

There are only a few reports of using CL-defined nanoparticle arrays. In previous research, RIE was used to generate 2D or 3D PS nonspherical colloidal particle arrays with a gas mixture of $CHF_3$ and $O_2$, and the resultant nonspherical particles could be used as novel building blocks for applications such as photonic crystals.[27,28] The morphology of the resultant nonspherical particles was similar to that of the upper layer of etched PS particles in this work. Nanopatterned metal layers also have been deposited via a combination of CL and RIE.[21,34] Furthermore, arrays of PS colloidal spheres with nanoholes were fabricated by selective etching of a colloidal monolayer partially embedded in an electrochemically deposited metal layer.[35]

In addition to the PS sphere and bottom silica nanoparticle sizes, the easily controllable parameters in this approach are the RIE conditions and the number of the spin-coating cycles. SEM images in Figure 3 give a demonstration of the flexibility of this approach for the formation of different morphologies of nanoparticle disks by changing the RIE duration and the number of spin-coating cycles with 1000 nm PS spheres on 50 nm silica nanoparticles. As shown in Figure 3A−F, the diameter of the nanoparticle disks was gradually reduced with an increase of the RIE duration. For a short RIE duration, close-packed nanoparticle disks are formed (Figure 3A,B). Each disk is connected to six nearest neighbors. A 4 min RIE duration was enough to remove the nanoparticles in the voids between the original PS spheres. The empty space was quasi-triangular, consistent with the opening between a triad of adjacent spheres. Increasing the RIE duration to 7 min, the nanoparticle disks were isolated and non-close-packed (Figure 3C,D) as a result of the etching of the PS spheres during the RIE. It is interesting that the circular shape of nanoparticle film at 7 min RIE was almost perfect. For additional RIE, the diameter of the nanoparticle disks was further reduced (Figure 3E,F). The circular disk shape for this longer RIE duration was not as well preserved. The transverse dimensions of the nanoparticle disks can be

(34) Choi, D.-G.; Kim, S.; Jang, S.-G.; Yang, S. M; Jeong, J.-R.; Shin, S.-C. *Chem. Mater.* **2004**, *16*, 4208.
(35) Yan, Q.; Liu, F.; Wang, L.; Lee, J. Y.; Zhao, X. S. *J. Mater. Chem.* **2006**, *16*, 2132.

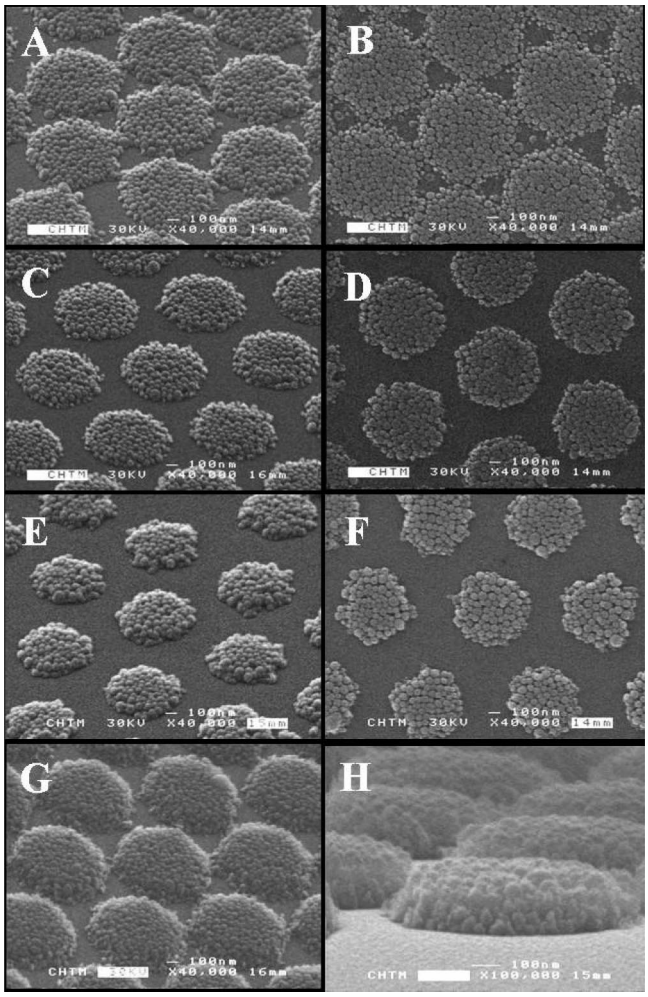


**Figure 3.** SEM images of nanoparticle patterns after different RIE durations with 1000 nm PS sphere CL: (A, B) 4 min, (C, D) 7 min, (E, F) 10 min, (G, H) 7 min, thick film.

readily controlled by the RIE duration, without changing the center-to-center distance of the nanoparticle disks which is set by the original CL process. The uniformity of nanoparticle film patterns over a large area has high fidelity to original uniformity of monolayer PS spheres (see Supporting Information Figure S2).

The thickness of the nanoparticle film was easily controlled in the spin-coating step. Thick nanoparticle disks (~200 nm) formed with two cycles of spin-coating and 7 min RIE are shown in Figure 3G,H. Even with same RIE condition as in Figure 3C,D, the disks were still partially connected due to the incomplete RIE of the thick nanoparticle film. The side wall of the disk is not vertical. Also, it is clear that the nanoparticle film was about four particles thick. With further RIE time, e.g. 10 min, we obtained the well-separated thick nanoparticle disks as expected (see Supporting Information Figure S3).

In addition to tuning the nanoparticle disk size without changing the period by controlling etching time and number of spin-coating cycles, the sizes of the colloidal particle in upper PS layer and bottom silica layer are also easy to change to generate different nanoparticle patterns. The SEM images in Figure 4 give examples of using small PS spheres (460 nm) atop a 50 nm diameter silica nanoparticle film. After the monolayer of 460 nm PS spheres was deposited on the silica nanoparticle film (see Figure 4A), 5 min RIE was used to etch the underlying silica nanoparticle film layer through the holes in the PS layer. With 5 min RIE, the 460 nm PS spheres were etched into small and isolated nonspherical PS particles (see Figure 4B). From a region that was destroyed in the sample preparation process, we further confirmed that the nanoparticle film was preserved well under protection of etched PS particles, and the outmost diameter of top etched PS particles was the same as the diameter of the resultant nanoparticle disk (see Figure 4C). After removal of PS particle, hexagonal arrays of nanoparticle disks of about 300 nm diameter were produced (see Figure 4D). The density of point defects using 460 nm PS spheres as "mask" was higher than that using 1000 nm PS spheres.

With a double-layered PS "mask", other types of nanoparticle patterns were fabricated. After deposition of double-layered 460 nm PS spheres atop 50 nm nanoparticle film (see Figure 4E), we employed the same RIE duration of 5 min as in the case of the monolayer of 460 nm PS sphere. The resultant nanoparticle patterns are shown in Figure 4F. During the RIE treatment of a doubled-layered "mask", PS spheres in both top layer and bottom layer are etched. Each PS sphere in top layer shrinks uniformly in all transverse directions while the PS spheres in the bottom layer are partially etched and do not change significantly due to masking by the top layer.[21] The shape and size of the double-layered arrays of etched PS particles change significantly with RIE duration.[28] If a relatively short RIE process was applied to the double-layered PS spheres, the shape of the nanoparticle patterns is expected to change from hexagonal to quasi-triangular shape.[28] With 5 min RIE, the final nanoparticle film has shallow quasi-triangular pits due to the thick double-layered as shown in Figure 4F. The RIE time for complete etching down to the metal layer in double-layered PS is longer compared to monolayer PS and even longer for a triple layer of PS. Additional flexibility in the resultant nanoparticle patterns is achieved with further RIE applied to multilayered PS spheres.[28]

To be successful with even smaller PS spheres as the masking layer, the underlying silica nanoparticles should also be smaller. Images in Figure 5 show results using 290 nm PS spheres atop 15 nm diameter silica nanoparticle films. A monolayer of 290 nm PS spheres was deposited on ~45 nm thick silica nanoparticle film (Figure 5A). RIE duration was 1.5 min for this case due to the smaller PS spheres and thinner silica nanoparticle film. After RIE etching and removal of the etched PS particles, hexagonal arrays of 15 nm nanoparticle disks were obtained as shown in Figure 5B,C. Even with only 1.5 min RIE, the nanoparticle disks were arranged in non-close-packed hexagonal patterns (see Supporting Information Figure S4). Moreover, in some regions of sample, the 290 nm PS spheres were deposited in a dense but random, non-close-packed monolayer. After RIE and removal of etched PS particles, a random, non-close-packed monolayer of silica nanoparticle disks was formed as expected (see Figure 5D). Patterns of nanoparticle disks have high fidelity to the patterns of upper layer. If other deposition methods such as layer-by-layer (LbL) are used

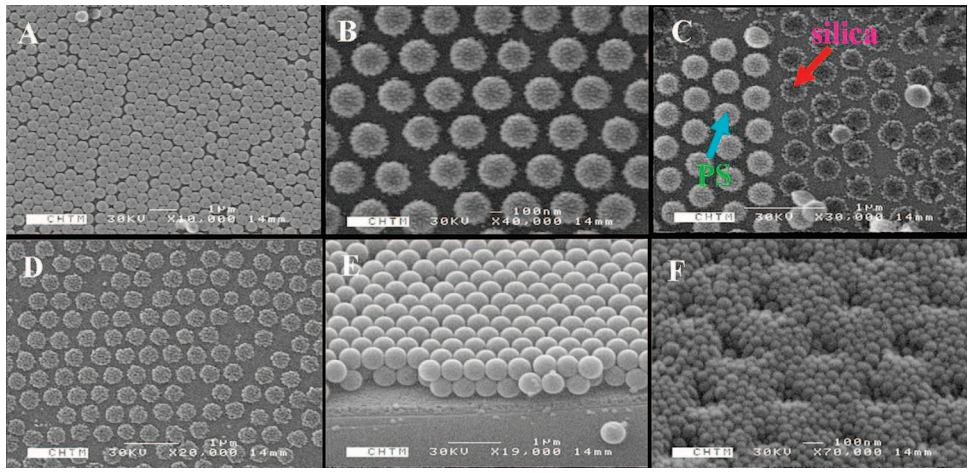


**Figure 4.** SEM images of 460 nm PS spheres on 50 nm silica nanoparticle film: (A) top view of a monolayer self-assembled PS sphere on silica nanoparticle film, (B, C) top view after 5 min RIE, (D) top view after removal of PS spheres, (E) side view of double-layer PS spheres atop a silica nanoparticle film, (F) tilted view (45°) of patterned nanoparticle films after 5 min RIE with double-layer PS spheres as a mask.

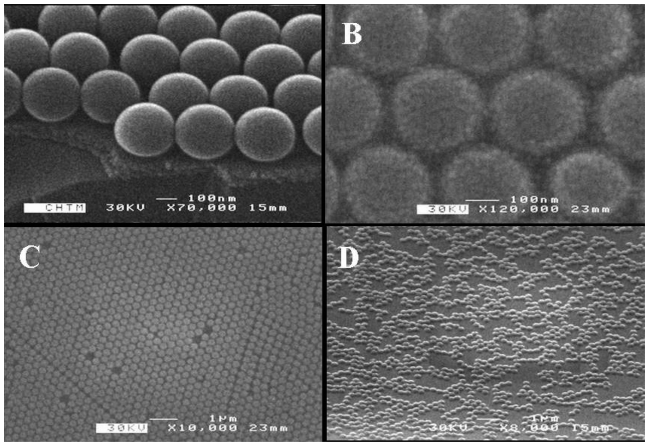


**Figure 5.** SEM images of 290 nm PS spheres atop a 15 nm silica nanoparticle film: (A) side view of self-assembled PS sphere on silica nanoparticle film, (B, C) top view after 1.5 min RIE and removal of monolayer PS spheres, (D) tilted view after 1.5 min RIE and removal of PS spheres with non-close-packed and randomly packed PS spheres as mask.

to form random or other types of PS patterns, more classes of patterns will be generated.

An important advantage of the two-particle approach is that we can easily define PS nanoparticle film patterns with silica spheres as the mask layer. First, a PS nanoparticle film is deposited on a bare Si substrate or a substrate with a thin layer of metal. In most cases, samples with a thin metal layer were used because the PS nanoparticle film patterns were not stable on samples without the thin metal layer. During the processing of the sample, a thin native silicon oxide may be formed, resulting in peeling off of the PS nanoparticle patterns during the removal of the silica spheres with a diluted HF solution.

After deposition of the PS nanoparticle film layer, large silica spheres were used to form the upper masking layer. An interesting observation is that the large silica spheres can creep underneath the nanoparticle film layer (see Supporting Information Figure S5). Even though we could deposit the PS nanoparticle film on a flat surface to form a large-area uniform film with only minor cracking (see Supporting Information Figure S6), it was difficult to deposit the large silica spheres on top of the PS nanoparticle film. Applying a short $O_2$ plasma treatment to the PS film before deposition of the large silica spheres to control the surface hydrophobicity resolved this issue and allowed successful deposition of the silica spheres over the PS nanparticle film. The purpose of $O_2$ plasma treatment is to modify the surface of the PS nanoparticles so that they become hydrophilic. The duration of $O_2$ plasma treatment was 0.12 min for 100 nm diameter PS nanoparticle film. As shown in Figure 6A, the spherical shape of the PS nanoparticles did not change much, but $O_2$ etching decreased the particle size, resulting in a separation between the initially close-packed particles. Large silica spheres (~520 nm) were easily deposited on top of this pretreated PS nanoparticle film as seen in Figure 6B. With further $O_2$ plasma treatment to the "large spheres" on "small spheres" film, we could etch through the interstices between the silica spheres (Figure 6C,D). The complete etching time depends mainly on the thickness of the PS nanoparticle film. $O_2$ plasma RIE does not etch the silica spheres in the top layer so that the top view of the resultant patterned PS nanoparticle film retains the initial silica sphere profile. After removal of silica spheres with diluted HF solution, we obtained the patterned PS nanoparticle film as shown in Figure 6E−H. Monolayer or double-layer hexagonal arrays of PS nanoparticle disks were achieved with different RIE times and different PS deposition conditions (Figure 6E,F). It was easy to form a monolayer PS nanoparticle film with the addition of a small amount polyvinylpyrrolidone (PVP).[32] For double layers, the top layer of PS nanoparticles was not close-packed due to the pretreatment etch, while the bottom PS nanoparticle layer was still close-packed. We also tested four-particle-thick PS nanoparticle films with spin-coating (Figure 6G,H). With different RIE time (0.6 and 1.2 min) for a thick PS film, the transverse pattern morphology was essentially unchanged, while the depth of etching increased with vertical profiles. We believe that we can easily fabricate nonspherical-particle patterned PS films using additional pre-etching. [28]

If we used the RIE with a gas mixture of $CHF_3$ and $O_2$, both the silica spheres and PS nanoparticles were etched, and the resultant etched profile was similar to the case of

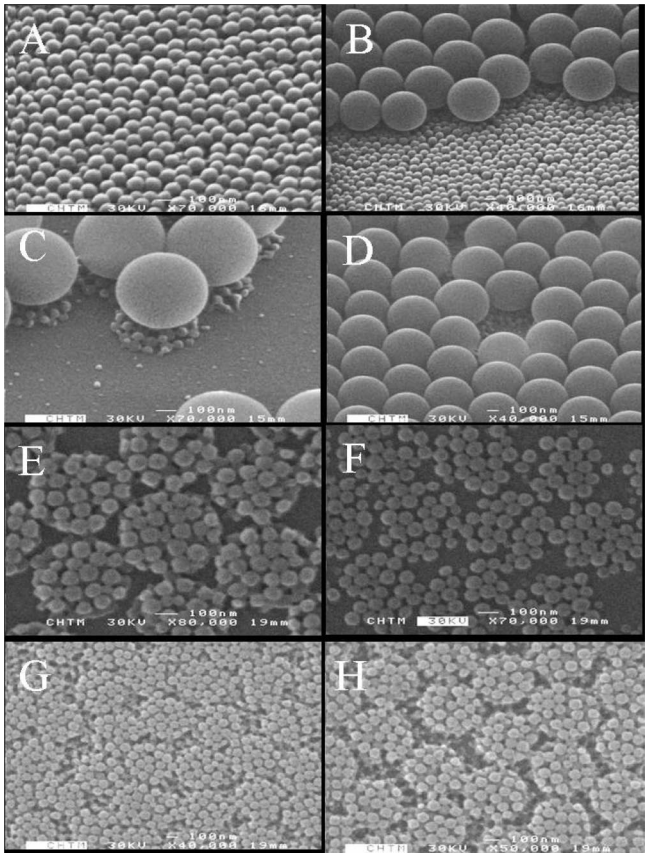


**Figure 6.** SEM images of a colloidal monolayer of 520 nm silica spheres atop 100 nm PS nanoparticle film after 0.12 min RIE pretreatment and RIE with $O_2$: (A) pretreatment 100 nm PS nanoparticle film with 0.12 min $O_2$ RIE; (B) a monolayer of self-assembled silica spheres on PS nanoparticle film; (C, D) after 0.6 min $O_2$ RIE, (E−H) after removal of silica spheres; (E) 1.0 min $O_2$ RIE; (F) 0.8 min $O_2$ RIE; (G) 0.6 min $O_2$ RIE; (H) 1.2 min $O_2$ RIE.

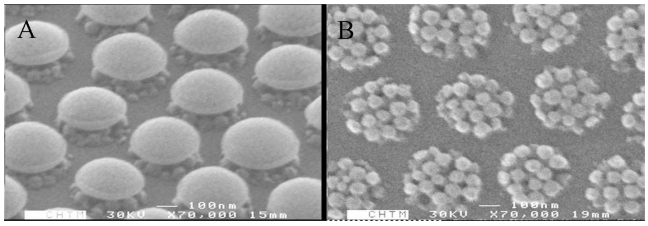


**Figure 7.** SEM images of a colloidal monolayer of 520 nm silica spheres on 100 nm PS nanoparticle film following 0.12 min RIE pretreatment and 6.2 min RIE using $CHF_3$ and $O_2$: (A) after RIE; (B) after removal of etched silica spheres.

PS on silica nanoparticle film discussed above (Figure 7). With enough RIE time (e.g., 6.2 min), hierarchical particle patterns with non-close-packed isolated and heterogeneous structures with inorganic and organic materials were achieved before removal of the upper layer (Figure 7A). Non-close-packed hexagonal arrays of PS nanoparticle islands were fabricated after removal of the silica spheres (Figure 7B). After the patterns of PS nanoparticle are formed, we could raise the temperature above the glass transition temperature ($T_g$) of the polystyrene (~93 °C)[36] to obtain smooth disks for applications such as microlenses.[37]

This method is applicable to other material systems if the appropriate deposition methods and etching conditions can be developed. For other kinds of materials (e.g., metal or semiconductor materials), it is critical to find suitable etching conditions for the underlying nanoparticle layer and removal methods to remove the upper large particle layer after the etching. As is demonstrated above, this method is easily extended to the nanoscale regime. Furthermore, we expect that this method is applicable to larger particles as well as long as the diameter of the large particles in the top layer is roughly 5 times larger than that of the small particles in the bottom layer.

With advances in the synthesis of nanoparticles, we expect that nonspherical particles can be used for the formation of more complex films. For example, after preparation of microrods with appropriate methods, the periodic rodlike patterns in nanoparticle film layer could be fabricated with self-assembled 2D microrod superlattices as an etch mask.[38,39]

This method is highly reliable. We could form excellent uniform, large-area (several $cm^2$) nanoparticle films via spin-coating from silica and PS nanoparticle suspensions. The thickness of nanoparticle film (to as thin as a monolayer) is easily controlled in spin-coating deposition step.[15] There are alternative well-developed deposition methods available for forming large-area, uniform monolayer or multiple-layer colloidal spheres crystals in this range of particle diameter.[30,40,41] With appropriate etching conditions, the pattern in the top-layer of microspheres is transferred easily to the underlying nanoparticle film.

Compared to our prior work on photolithographically defined nanoparticle patterns,[11,12,14] the current work has the following distinctions: (1) It is a low-cost and simple process as the upper layer is formed by self-assembly of large particles instead of photolithography; this eliminates the most expensive steps of our previous work (the laser system); the tradeoff is a reduced pattern flexibility. (2) The diameter of nanoparticle patterns can be accurately tuned by adjusting the etch duration while the period is kept constant due to the self-assembly morphology and the spherical shape of large particles; in contrast, in the photolithography method, it is not possible to control the dimension of patterns by adjusting the etch process as the photoresist patterns have vertical side walls. (3) This technique is readily extensible to other material systems as demonstrated above using silica materials for the top layer, while for photolithography, the top layer is always a polymer (photoresist). Thus, there are more choices for the bottom layer of nanoparticle materials and more types of hierarchical particle arrays with different combinations of particles. In all cases, it is necessary to find suitable etch and selective mask removal processes.

(36) Gates, B.; Park, S. H.; Xia, Y. *Adv. Mater.* **2000**, *12*, 653.
(37) Lu, Y.; Yin, Y.; Xia, Y. *Adv. Mater.* **2001**, *13*, 34.
(38) Alargova, R. G.; Bhatt, K. H.; Paunov, V. N.; Velev, O. D. *Adv. Mater.* **2004**, *16*, 1653.
(39) Mohraz, A.; Solomon, M. J. *Langmuir* **2005**, *21*, 5298.
(40) Kitaev, V.; Wong, S.; Ozin, G. A. *J. Am. Chem. Soc.* **2003**, *125*, 15589.
(41) Yan, Q.; Zhou, Z.; Zhao, X. S. *Langmuir* **2005**, *21*, 3158.

## Conclusions

We report a simple approaching for fabricating hierarchical particle arrays and mesoscopic colloidal nanoparticle patterns using two-step self-assembly, reactive-ion etching (RIE), and selective removal of the CL mask layer. Both silica and PS nanoparticle films with hexagonal patterns were demonstrated under different RIE conditions. The distances between isolated film regions are held constant while the diameter of the nanoparticle film disks is easily tuned with the RIE conditions. More types of patterns can be achieved by varying the thickness of large particle layer, crystal orientation, RIE conditions, and postprocessing steps. The technique can be useful in the fabrication of 2-D periodic nanoparticle film arrays in a non-close-packed configuration. New optical and catalytic properties will be explored on these patterned nanoparticle films. Moreover, these patterned nanoparticle film will find technological applications in biosensors and micro- and nanodevices as well as using them as templates for further fabrication.

**Acknowledgment.** This work was supported by the National Science Foundation under Grant 0515684.

**Supporting Information Available:** SEM images of more detailed CL-defined patterns. This material is available free of charge via the Internet at http://pubs.acs.org.

CM702644C